

Antitumour activity of TH1579, a novel MTH1 inhibitor, against castration-resistant prostate cancer

MINGQIU HU, JING NING, LIKAI MAO, YUANYUAN YU and YU WU

Department of Urology, The Second Affiliated Hospital of Bengbu Medical College, Bengbu, Anhui 233040, P.R. China

Received June 13, 2020; Accepted November 2, 2020

DOI: 10.3892/ol.2020.12324

Abstract. Castration-resistant prostate cancer (CRPC) treatment still remains difficult. The aim of the present study was to determine the antitumour efficacy of the MutT homolog 1 (MTH1) inhibitor, TH1579, against castration-resistant prostate cancer. PC-3 and DU-145 prostate cancer cells were treated with different concentrations of TH1579. C4-2 cells with or without androgen receptor (AR) were also treated with TH1579 to assess AR function. Cell survival, 8-oxo-dG levels and DNA damage were measured using cell viability assays, western blotting, immunofluorescence analysis and flow cytometry. TH1579 inhibited CRPC cell proliferation in a dose-dependent manner. The viabilities of PC-3 and DU-145 cells treated with 1 μ M of TH1579 were 28.6 and 24.1%, respectively. The viabilities of C4-2 cells with and without AR treated with 1 μ M TH1579 were 10.6 and 19.0%, respectively. Moreover, TH1579 treatment increased 8-oxo-dG levels, as well as the number of 53BP1 and γ H2A.X foci, resulting in increased DNA double-strand breakage and apoptosis in PC-3 and DU-145 cells. The findings of the present study demonstrated that TH1579 exerted strong antitumour effects on CRPC cells, and may therefore be used as a potential therapeutic agent for the clinical treatment of CRPC.

Introduction

Prostate cancer is the leading type of non-skin cancer and the fifth leading cause of cancer-associated death among men in the United States, as well as a major public health burden worldwide (1). Most prostate cancers are initially sensitive to androgen deprivation treatment; however, they

progress to a castration-resistant state after a median interval of 18-24 months (2,3). While cytotoxic compounds such as docetaxel are effective against castration-resistant prostate cancer (CRPC), they may produce dose-limiting toxicity in normal tissues (2). Currently, there is no effective treatment that substantially improves the overall survival of patients with CRPC (2).

Several studies have demonstrated a positive association between cancer and the imbalance of redox homeostasis and/or increased levels of reactive oxygen species (4,5), which oxidise nucleobases in the free deoxynucleotide triphosphate (dNTP) pool. High levels of 8-oxo-dG, a major product of reactive oxygen species-induced cellular damage (5), can promote apoptosis and inhibit cellular proliferation (5). Accordingly, the incorporation of oxidised 8-oxo-dG into DNA can suppress tumour growth (6). Human MutT homolog 1 (MTH1, also known as Nudix hydrolase 1) hydrolases have been shown to oxidise purine dNTPs and prevent their incorporation into DNA (7). Previous studies have also revealed that the levels and catalytic activity of MTH1 are increased in multiple cancer cell lines (8) and certain surgical specimens, including lung cancer (9), brain tumours (10,11), renal (12), breast (13), colorectal (14) and oesophageal cancer (15). MTH1 overexpression inhibits reactive oxygen species-induced DNA damage and premature senescence (16). Based on these findings, MTH1 has been suggested as a potential drug candidate for cancer treatment. Studies (8,17,18) revealed that MTH1 prevents the incorporation of oxidised dNTPs, such as 8-oxo-dG, into DNA and inhibits cell death. Although MTH1 is not essential in normal cells (8), it is required by cancer cells for survival, independent of their tissue origin (8,18).

By contrast, some researchers have argued that certain MTH1 inhibitors do not suppress proliferation and induce apoptosis in certain human cancer cell lines (19,20). The underlying reason is presumed to be off-target interaction of the MTH1 inhibitors with tubulin instead of MTH1 (21). To address this controversy, studies (18,22-24) have discovered a novel compound, TH1579. Compared with previously characterised MTH1 inhibitors, TH1579 showed higher potency (sub-nanomolar concentration) and more selective MTH1 inhibition, with good oral bioavailability. In recent studies (25,26), TH1579 also showed excellent pharmacokinetic and antitumour effects in chemotherapy-resistant patient-derived malignant melanoma and human melanoma

Correspondence to: Dr Mingqiu Hu, Department of Urology, The Second Affiliated Hospital of Bengbu Medical College, 220 Hongye Road, Bengbu, Anhui 233040, P.R. China
E-mail: humingqiu@me.com

Abbreviations: MTH1, MutT homolog 1; CRPC, castration-resistant prostate cancer; dNTP, deoxynucleotide triphosphate; DSB, double-strand break; AR, androgen receptor

Key words: MTH1, CRPC, 8-oxo-dG, antitumour

mouse xenograft models (25,26). TH1579 prevents the accumulation of 8-oxo-dG and induces DNA damage and cell apoptosis without off-target interaction with tubulin (26). Additionally, recent evidence suggests that TH1579 inhibits MTH1 activity in glioblastoma and glioblastoma stem cells *in vitro* and *in vivo* (23), thus indicating that MTH1 may act as a potential anticancer target.

Although recent studies have demonstrated that MTH1 inhibitors are effective against gastric (27), liver (24) and bladder (28) cancers, the antitumour efficacy of MTH1 inhibitors against CRPC is not known. Moreover, some studies (8,18) have discussed the probable cytotoxic effects of MTH1 inhibitors on human prostate cancers, including CRPC. The aim of the present study was to determine the antitumour efficacy of TH1579 against CRPC, and to investigate the underlying molecular mechanism of MTH1 inhibitors. Furthermore, the potential clinical use of MTH1 inhibitors against CRPC was investigated.

Materials and methods

Cell culture. Human prostate cancer cell lines (PC-3, DU-145 and C4-2) (all Procell Life Science & Technology Co., Ltd.) were cultured in RPMI-1640 medium (Thermo Fisher Scientific, Inc.) supplemented with 10% foetal bovine serum (Thermo Fisher Scientific, Inc.) and penicillin-streptomycin (90 U/ml) at 37°C (5% CO₂) in a humidified atmosphere. The cells were cultured in T-75 flasks and passaged by trypsinisation at ~70% confluence.

TH1579 treatment and assessment of cell viability. Cells were seeded into 96-well plates at a density of 6×10^4 /ml (3×10^3 cells/50 μ l/well). After 24 h of incubation in a humidified incubator (37°C, 5% CO₂), the cells were treated with TH1579 (HPLC purity, >98%) purchased from ProbeChem®, and incubated for an additional 72 h at 37°C and 5% CO₂. TH1579 was serially diluted to generate the following final concentrations: 0.0625, 0.125, 0.250, 0.50 and 1.0 μ M. Each concentration of TH1579 was tested in triplicate (3 wells/TH1579 concentration), and dimethyl sulfoxide (DMSO) was used as the negative control. The reaction was terminated by the addition of 100 μ l resazurin dye solution (400 μ l in 20 ml; Sigma-Aldrich; Merck KGaA) to each well, followed by further incubation for 2-3 h. Cell viability was determined by measuring the absorbance using the Hidex Sense microplate reader (Hidex Oy). In viable cells, the amount of oxidised resazurin (blue colour) is low, and that of reduced resazurin is high (pink-red colour). Therefore, viable cells fluoresce pinkish-red after a 2-h incubation, whereas dead cells fluoresce blue.

Androgen receptor (AR) silencing. For this experiment, 1×10^5 C4-2 cells (cat. no. GOY0197) which were previously inoculated with AR-targeted doxycycline-inducible short hairpin (sh)RNA (synthesized by Goybio), were seeded into each well of a 6-well plate and allowed to attach for 24 h. Doxycycline (1 μ g/ml) was added to each well and the cells were incubated for a further 72 h prior to experimentation. The synthesis of the shRNA construct, comprising AR-specific shRNA inserted in a doxycycline-inducible FHI1UTG lentiviral vector, has been previously described (8).

Western blot analysis

Preparation of cell lysates for protein extraction. PC-3 or DU-145 cells were seeded into 6-well plates (4×10^5 cells/well). After 12-20 h of incubation, the cells were treated with DMSO, TH1579 (0.5 and 1 μ M) or etoposide (1 μ M), and then incubated for 24 h. The cells were then harvested on ice, washed once with cold PBS, trypsinised and centrifuged at 450 x g for 5 min at 25°C. After two more washes and centrifugation cycles, 50-100 μ l lysis buffer solution [1 ml lysis buffer solution=890 μ l Lysis buffer, 100 μ l protease inhibitor (10X; both Roche Diagnostics) and 10 μ l of phosphatase inhibitor (100X; Thermo Fisher Scientific, Inc.)] was added to each cell pellet, followed by incubation on ice for 30 min. Whole-cell lysates were sonicated for 1 min and centrifuged at 12,000 x g and 4°C for 30 min to solubilise all proteins.

Determination of protein concentration. The supernatant from the whole-cell lysates were transferred to new tubes, and the protein concentration of each sample was determined using a Pierce™ BCA protein assay kit (Thermo Fisher Scientific, Inc.).

Gel electrophoresis and western blotting. To load 20 μ g protein per well, each sample was mixed with Laemmli SDS-PAGE sample buffer (Bio-Rad Laboratories, Inc.) at a 3:1 ratio. The samples were heated at 95°C for 5 min, loaded onto 12-well Mini-PROTEAN TGX precast gels (Bio-Rad Laboratories, Inc.) and electrophoresed at 120 V for ~1.5 h. The samples were subsequently transferred onto a polyvinylidene difluoride membrane (cut into three strips for protein with different molecular weights: Low, medium, and high), which was then incubated with Odyssey blocking buffer (LI-COR Biosciences) for 30 min at 25°C. After blocking, the membrane was incubated at 4°C overnight with primary antibodies in blocking buffer. The following antibodies were used: Mouse polyclonal anti-H2A.X (1:1,000; cat. no. 05636; EMD Millipore), rabbit monoclonal anti-histone H3 (1:1,000; cat. no. ab1791; Abcam), rabbit polyclonal anti-cleaved poly (ADP-ribose) polymerase (cPARP; 1:1,000; cat. no. 9541; Cell Signaling Technology, Inc), rabbit monoclonal anti-p-p53 (S15; 1:1,000; cat. no. 9284; Cell Signaling Technology, Inc.) and mouse monoclonal anti- β actin (1:10,000; cat. no. ab6276; Abcam). After overnight incubation, the membrane was washed three times with TBS-Tween 20 (1:20 TBST; 10 min/wash) and incubated with IRDye-conjugated donkey anti-rabbit and donkey anti-mouse fluorescence secondary antibodies (1:5,000; cat. nos. 925-68073 and 926-32212; LI-COR Biosciences) in TBST at 25°C for 30 min in the dark. The membrane was subsequently washed three times with TBST (10 min/wash), and the protein bands were visualised using the LI-COR Odyssey imaging system (LI-COR Biosciences).

Flow cytometric analysis. PC-3 or DU-145 cells (1×10^6 /ml) were seeded into 25-cm² flasks at 25°C, treated with TH1579 compounds, and harvested after 72 h. The cells were washed twice with PBS, resuspended in 1X binding buffer and centrifuged at 450 x g after mixing. The pellets were resuspended in a solution of FITC-Annexin V (Thermo Fisher Scientific; cat. no. A23204 and propidium iodide (PI; BD Biosciences; 900 μ l 1X binding buffer +45 μ l FITC-Annexin V +45 μ l of PI for

8 samples; 110 μ l/sample). After gentle vortexing, the solution was incubated at 25°C for 15 min in the dark. Subsequently, 400 μ l 1X binding buffer was added to each sample, and the sample mixture was transferred to new tubes within 15 min for flow cytometric analysis using the FACSCalibur Instrument (Becton, Dickinson and Company). The data were analysed using BD FACS Diva and CellQuest Pro software (cat. no. 643274; cat.no. Rev. A; both from BD Biosciences).

Immunofluorescence analysis. DU-145 or PC-3 cells (2.5×10^5) were seeded onto glass coverslips in a 6-well plate, and incubated for 24 h before treatment with DMSO, TH1579 (0.5 and 1 μ M) or etoposide (1 μ M); the cells were then incubated for an additional 24 h, washed twice with 1X PBS, and fixed in 1 ml 4% paraformaldehyde in PBS +0.1% Triton X (PBS-T) at room temperature for 20 min. The fixed cells were rinsed twice with PBS for 10 min each, permeabilised with PBS +0.5% Triton X for 15 min, blocked with 3% BSA (Thermo Fisher Scientific, Inc.) in PBS-T for 1 h, and incubated at 4°C overnight with primary antibodies diluted in 3% BSA in PBS. The following primary antibodies were used: Mouse anti- γ H2AX^{Ser139} (1:1,000; cat. no. 05-636; EMD Millipore;) and rabbit anti-p53-binding protein 1 (53BP1; 1:1,000; cat. no. ab36823; Abcam). After overnight incubation, the cells were rinsed three times with PBS-T for 10 min and incubated with fluorophore-conjugated donkey anti-rabbit IgG AlexaFluor488 and donkey anti-mouse IgG AlexaFluor555 secondary antibodies (1:500 in blocking solution; cat. no. R37118 and A32773; both from Molecular Probes; Thermo Fisher Scientific, Inc.) at room temperature for 1 h in the dark. DNA was counterstained with DAPI (1:1,000; ATTO-TEC GmbH) in 1X PBS. Coverslips were mounted onto glass slides with one drop of ProLong Gold Antifade Reagent (Invitrogen; Thermo Fisher Scientific, Inc.) and dried overnight.

Each slide was imaged using an LSM 780 confocal laser scanning microscope (Zeiss GmbH) with a planachromat 63x/NA 1.4 oil immersion objective at excitation wavelengths of 543 and 633 nm. A total of 10 random fields were imaged for each slide and, subsequently, the cells in each field were counted. The expression of the DNA damage marker γ H2AX was determined by counting cells with 53BP1 foci (a cell with ≥ 9 53BP1 foci was considered to be positive) and γ H2AX foci; 10 field images were acquired to calculate the mean for each treatment condition.

Determination of 8-oxo-dG levels. DU-145 or PC-3 cells (2.5×10^5) were seeded onto glass coverslips in a 6-well plate, incubated for 24 h before treatment with DMSO or TH1579 (0.5 and 1 μ M), and incubated for an additional 24 h. For the positive control, 50 mM potassium bromate was added to one well 1 h before harvesting the cells. The harvested cells were washed twice with 1X PBS and fixed in chilled methanol/acetone (1:1) for 30 min at -20°C. The fixed cells were rinsed twice with 1X PBS for 10 min each, followed by denaturation with 2.5 normal concentration (N) HCl at room temperature for 45 min. Thereafter, cells were rinsed thrice with 1X PBS on a shaker for 5 min each, and neutralised with 0.1 M Na₂BO₄O₇ (pH 8.8) for 10 min. The cells were again rinsed thrice with 1X PBS on a shaker for 5 min each, and

then permeabilised with 0.5% Triton X-100 in PBS for 15 min. After rinsing thrice with 1X PBS for 5 min, the cells were blocked with 4% BSA in PBS for 1 h and incubated at 4°C overnight with mouse anti-8 hydroxyguanosine (1:200; cat. no. ab48508; Abcam) primary antibody.

After overnight incubation, the cells were rinsed thrice with PBS-T for 10 min and incubated with fluorophore-conjugated donkey anti-mouse IgG AlexaFluor488 secondary antibody (1:500 in blocking solution; cat. no. A32766; Thermo Fisher Scientific, Inc.) at room temperature for 1 h in the dark. DNA was counterstained with DAPI (1:1,000) prepared in 1X PBS. The coverslips were mounted onto the slides with one drop of ProLong Gold Antifade Reagent and dried overnight. The slides were then imaged as aforementioned (*Immunofluorescence analysis* section), and 8-oxo-dG levels were quantified using an in-house software based on ImageJ from National Institutes of Health (DAPI was used as a marker of nuclear DNA).

Colony formation assay. For the colony formation assay, 500 cells in 10 ml medium were seeded into a 10-cm² dish. The cells were treated with different concentrations of inhibitors (10 μ l/dish) after incubation at 37°C for 5 h; the culture medium was changed after every 72 h. On day 10, the colonies were fixed and stained with methylene blue (4 g/l) in methanol and visualised manually for 30 min at 25°C. A group of 30-50 cells was considered to be a colony and counted using a colony counter (aCOLade; Synbiosis; Synoptics Ltd.). Surviving fractions were calculated by comparison with DMSO-treated control cells.

Statistical analysis. Multiple comparisons between groups were performed with Tukey's test using GraphPad Prism 6 (GraphPad Software, Inc.). All the experiments were repeated for three times. Data are presented as the mean \pm SEM, and $P < 0.05$ was considered to indicate a statistically significant difference.

Results

TH1579 inhibits prostate cancer cell proliferation in a dose-dependent manner. The efficacy of the MTH1 inhibitor, TH1579, was determined using PC-3, DU-145 and C4-2 prostate cancer cell lines. In the present study, TH1579 was found to effectively kill both hormone-dependent and CRPC cells (Fig. 1A-C). The viabilities of PC-3, DU-145 and C4-2 (AR +/-) cells treated with 0.25, 0.5 and 1 μ M TH1579 were lower than those of cells in the DMSO control group ($P < 0.05$). The viabilities of PC-3 and DU-145 cells treated with 1 μ M TH1579 were 28.6 and 24.1%, respectively. The viabilities of C4-2 cells with and without AR treated with 1 μ M TH1579 were 10.6 and 19.0%, respectively. Moreover, the viability of the C4-2 cells was not notably different between 1 and 0.5 μ M TH1579 treatment.

A colony formation assay was performed to determine the proliferation capacity of cells treated with TH1579 (Fig. 1C and D). The number of colonies from both prostate cancer cells treated with all concentrations of TH1579 was significantly lower ($P < 0.05$) than that of the DMSO-treated control cells. However, the number of DU-145 cell colonies

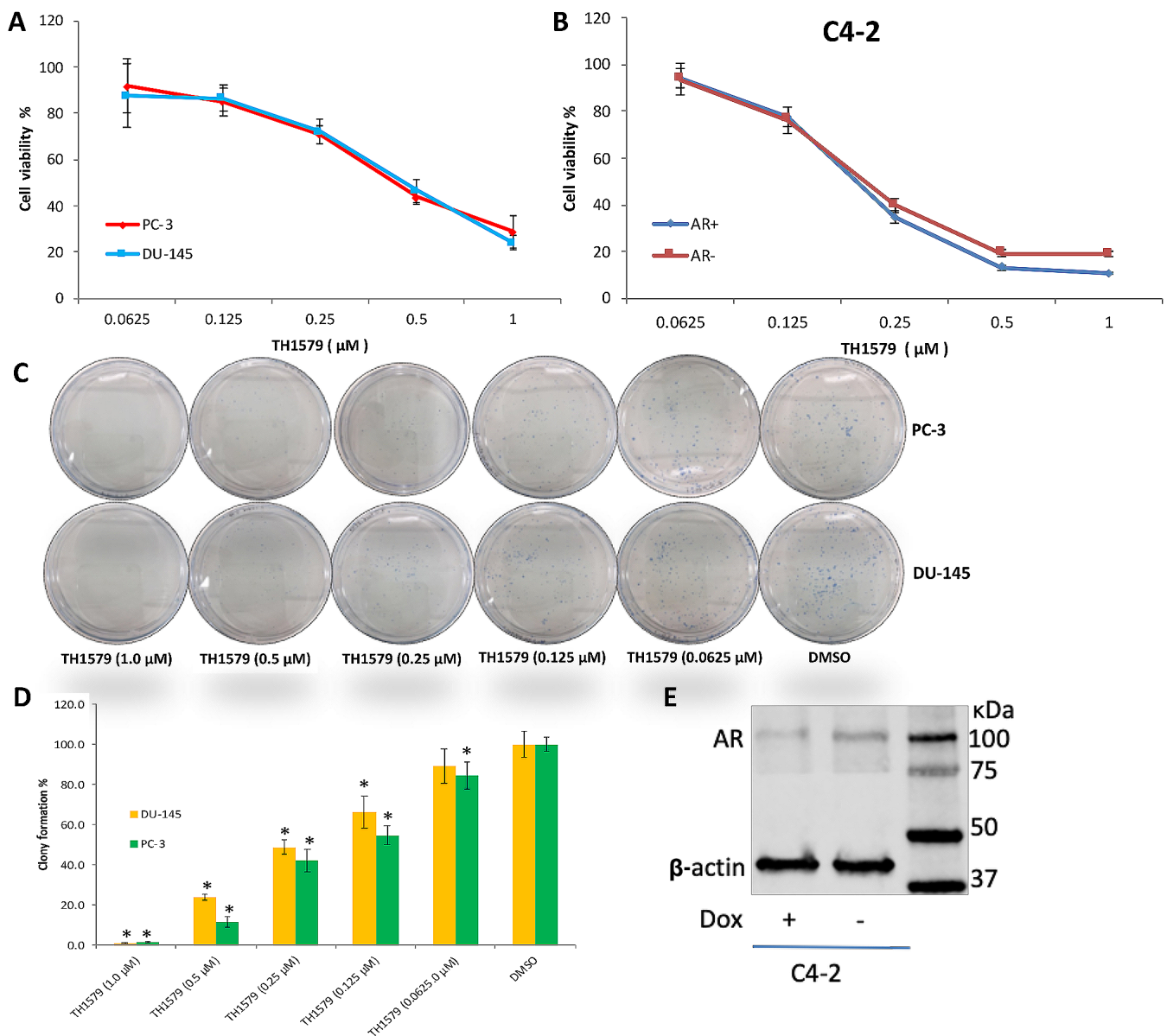


Figure 1. TH1579 inhibits the proliferation of prostate cancer cells in a dosage-dependent manner. Cellular viability assays were performed to show the percentage of (A) PC-3, DU-145 and (B) C4-2 (AR+/-), cells treated with a series concentration of TH1579 for 72 h relative to cells in the DMSO control group. Data are presented as the mean \pm SEM of >3 independent experiments. (C) Representative images of PC-3 and DU-145 cell colony formation 10 days after treatment with TH1579. (D) Quantification of clonogenic survival of DU-145 and PC-3 cells 10 days after treatment with TH1579. Values represent the percentage of colonies relative to DMSO-treated controls displayed as the mean \pm SEM of three independent experiments. * $P < 0.01$, each experiment group [including TH1579 (1.0 μ M), TH1579 (0.5 μ M), TH1579 (0.25 μ M), TH1579 (0.125 μ M), TH1579 (0.0625 μ M)] vs. DMSO group, Tukey's test. (E) Western blot confirmation that C4-2 cell AR expression was suppressed after incubation with Dox (1 μ g/ml) for 72 h. AR, androgen receptor; Dox, doxycycline.

treated with 0.0625 μ M TH1579 was comparable to that of DMSO-treated cells (Fig. 1D). Therefore, the results indicated that TH1579 inhibited CRPC cell proliferation in a dose-dependent manner.

Western blotting was then performed to determine whether incubation of C4-2 cells with doxycycline for 3 days inhibits AR activity. The results suggested that the expression of AR in C4-2 cells was significantly inhibited by doxycycline (Fig. 1E).

TH1579 induces apoptosis in CRPC cells. To further understand the underlying mechanism of the antitumour activity of TH1579 on CRPC cells, flow cytometry and western blotting were performed. Flow cytometric analysis showed that the rate of apoptosis in PC-3 and DU-145 cells treated with TH1579

for 72 h was significantly higher than that in DMSO-treated control cells (only late apoptosis were assessed in the experiment; Fig. 2A and B). Western blotting revealed that the expression of apoptotic protein markers such as cPARP and γ H2A.X was upregulated in these cells (Fig. 2C). Moreover, the expression of p53 (S15) was downregulated in PC-3 cells, owing to p53 deletion (29).

MTH1 inhibition promotes the incorporation of 8-oxo-dG into CRPC cells. An immunofluorescence assay was performed to determine the extent of 8-oxo-dG incorporation into the DNA of CRPC cells (Fig. 3A and B). As shown in Fig. 3C and D, the level of 8-oxo-dG in PC-3 or DU-145 cells treated with TH1579 for 72 h was significantly higher than that in the

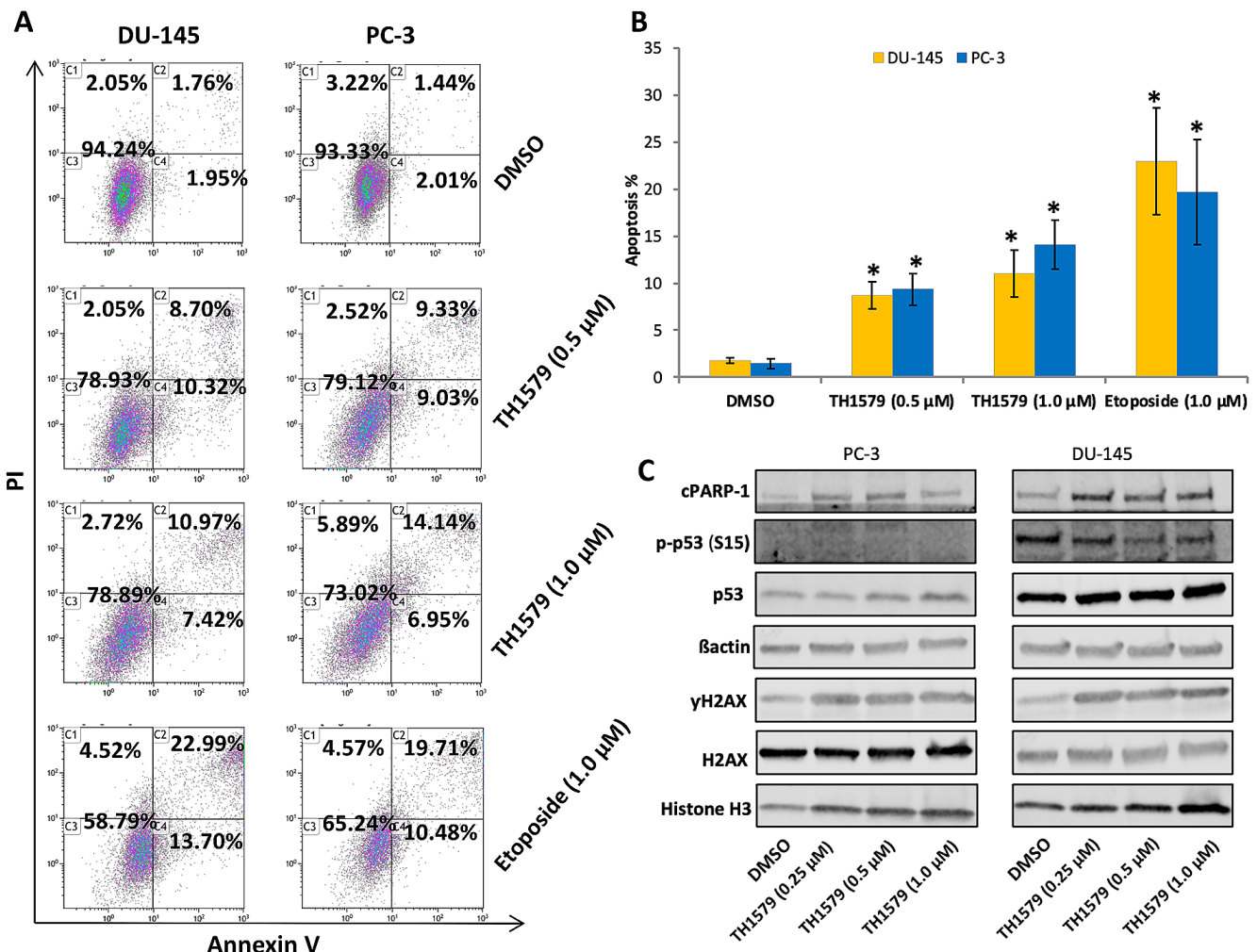


Figure 2. TH1579 induces apoptosis in castration-resistant prostate cancer. (A) Representative images of flow cytometric analysis highlighting apoptosis in DU-145 and PC-3 cells treated with TH1579 for 72 h. (B) Flow cytometric quantification of apoptosis in PC-3 or DU-145 cells following PI and Annexin V staining. Values represent the mean \pm SEM from three independent experiments. * P <0.01, each experiment group [including TH1579 (1.0 μ M), TH1579 (0.5 μ M) or Etoposide group vs. DMSO group]; Tukey's test. (C) Representative western blot images of cPARP-1, p-p53 (S15) and γ H2A.X expression levels from >3 independent experiments 24 h after incubation with TH1579. cPARP-1, cleaved poly (ADP-ribose) polymerase 1; PI, propidium iodide.

DMSO-treated control cells (P <0.05). These results indicated that TH1579 inhibits the enzymatic activity of MTH1.

TH1579 promotes DNA double-strand breakage in CRPC cells. The accumulation of 8-oxo-dG in DNA can increase DNA double-strand breaks (DSBs) (4). 53BP1 is an important regulator of the cellular response to DNA DSBs and promotes end-joining of distal DNA ends (7). Phosphorylation of histone H2AX at a serine four residues from the carboxyl terminus (to form γ H2AX) is considered to be a sensitive marker for DNA DSBs. γ H2AX can also detect low levels of DNA damage (8,18). To quantify DNA damage in PC-3 and DU-145 cells treated with TH1579 for 72 h, these cells were stained with anti-53BP1 and anti- γ H2AX antibodies. Immunofluorescence analysis revealed the accumulation of 53BP1 and γ H2AX nuclear foci (Fig. 4A and B). Furthermore, confocal microscopy revealed that the number of 53BP1 and γ H2AX nuclear foci in CRPC cells treated with 1 μ M TH1579 was significantly greater than that in DMSO-treated cells (Fig. 4C and D). These results provided substantial evidence that TH1579 inhibited MTH1 activity and induced DNA damage.

Discussion

Prostate cancer is a leading cause of mortality and morbidity among men. Although extensive attempts have been made to improve the understanding of the underlying mechanism of CRPC and its treatment efficiency (1-3,30-33), the clinical treatment of CRPC remains a challenge. The high heterogeneity of prostate cancer makes clinical stratification and selection of appropriate treatment strategies difficult (1,2). Therefore, effective therapeutic strategies for CRPC are required to improve the overall survival of patients. To the best of our knowledge, the present study is the first to determine the antitumour effects and underlying molecular mechanisms of the MTH1 inhibitor, TH1579, in human prostate cancer cells.

In the present study, cell viability and colony formation assays were performed to demonstrate that TH1579 exhibits antitumour activity against PC-3 and DU-145 cells in a dose-dependent manner. Previous studies have shown that TH1579 exerts antitumour activity against osteosarcoma, colorectal cancer, drug-resistant bladder cancer, glioblastoma

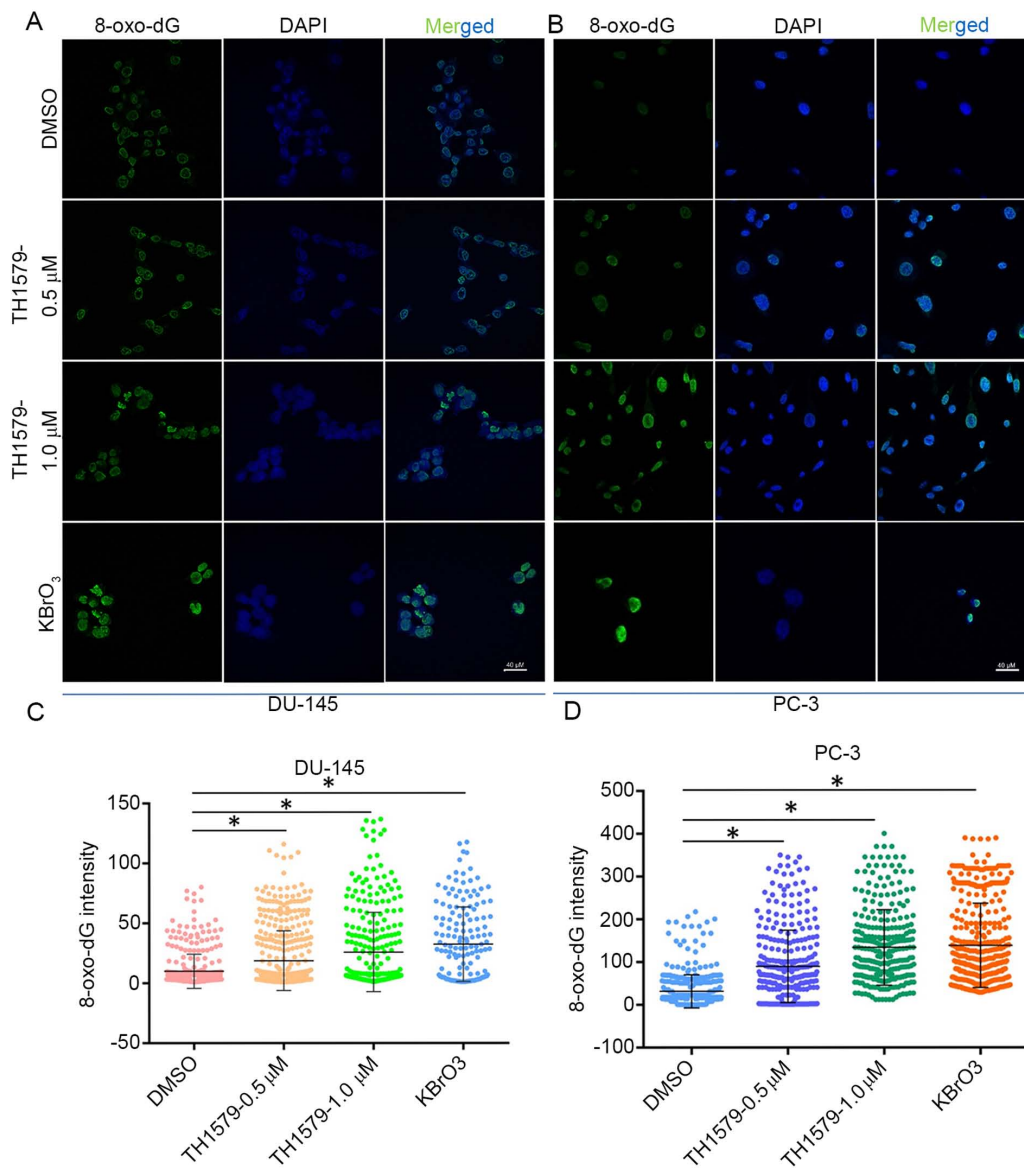


Figure 3. TH1579 promotes 8-oxo-dG incorporation into castration-resistant prostate cancer cells. Representative immunofluorescence images of 8-oxo-dG accumulation in (A) DU-145 and (B) PC-3 cells after incubation with TH1579 for 72 h. Quantification of 8-oxo-dG intensity in (C) DU-145 and (D) PC-3 cells after 72 h treatment with TH1579 or KBrO₃. Data are shown as the mean \pm SEM from three independent experiments; ≥ 200 cells/sample. * $P < 0.01$, Tukey's test. KBrO₃, potassium bromate.

and hepatic cancer cells both *in vitro* and *in vivo* (18,23,24). In these studies, TH1579 increased 8-oxo-dG levels, as well as the number of γ H2AX and 53BP1 nuclear foci (DNA damage markers), and decreased the size of xenograft tumours in mice *in vivo*. The present study presented evidence supporting the use of TH1579 as a therapeutic target for CRPC. Immunofluorescence assay results showed that TH1579 treatment increased 8-oxo-dG levels and promoted 53BP1 and γ H2A.X foci formation in prostate cancer cells. Moreover, flow cytometry assays indicated that TH1579 treatment increased the rate of apoptosis and decreased the viability of DU-145 and PC-3 cells. These findings are in agreement with those of previous studies (18,23,24). Considering these points, this MTH1 inhibitor may be beneficial as a novel clinical treatment against CRPC. However, further *in vivo* studies are required to confirm the clinical efficacy of the compound without unacceptable off-target toxicity.

Although the antitumour activity of TH1579 on cancer cells is well known, the underlying mechanism is not clear (18). A previous study suggested that the MTH1 inhibitors TH588 or TH287 exhibit antitumour activity by targeting tubulin, but not MTH1 (8). However, Warpman Berglund *et al* (18) demonstrated that these MTH1 inhibitors are not fully effective due to their inability to incorporate 8-oxo-dG into the DNA. In the present study, accumulation of 8-oxo-dG in cellular DNA was observed after treatment with TH1579 for 72 h. Simultaneously, increased 53BP1 and γ H2AX foci formation in PC-3 and DU-145 cells was also observed. These findings suggested that TH1579 can induce CRPC cell apoptosis and suppress cancer cell proliferation by targeting MTH1.

TH1579 killed both AR-expressing and AR-deficient C4-2 cells, indicating that the antitumour activity of TH1579 was independent of AR signalling. However, a previous study (34) proposed that AR signalling is essential for the

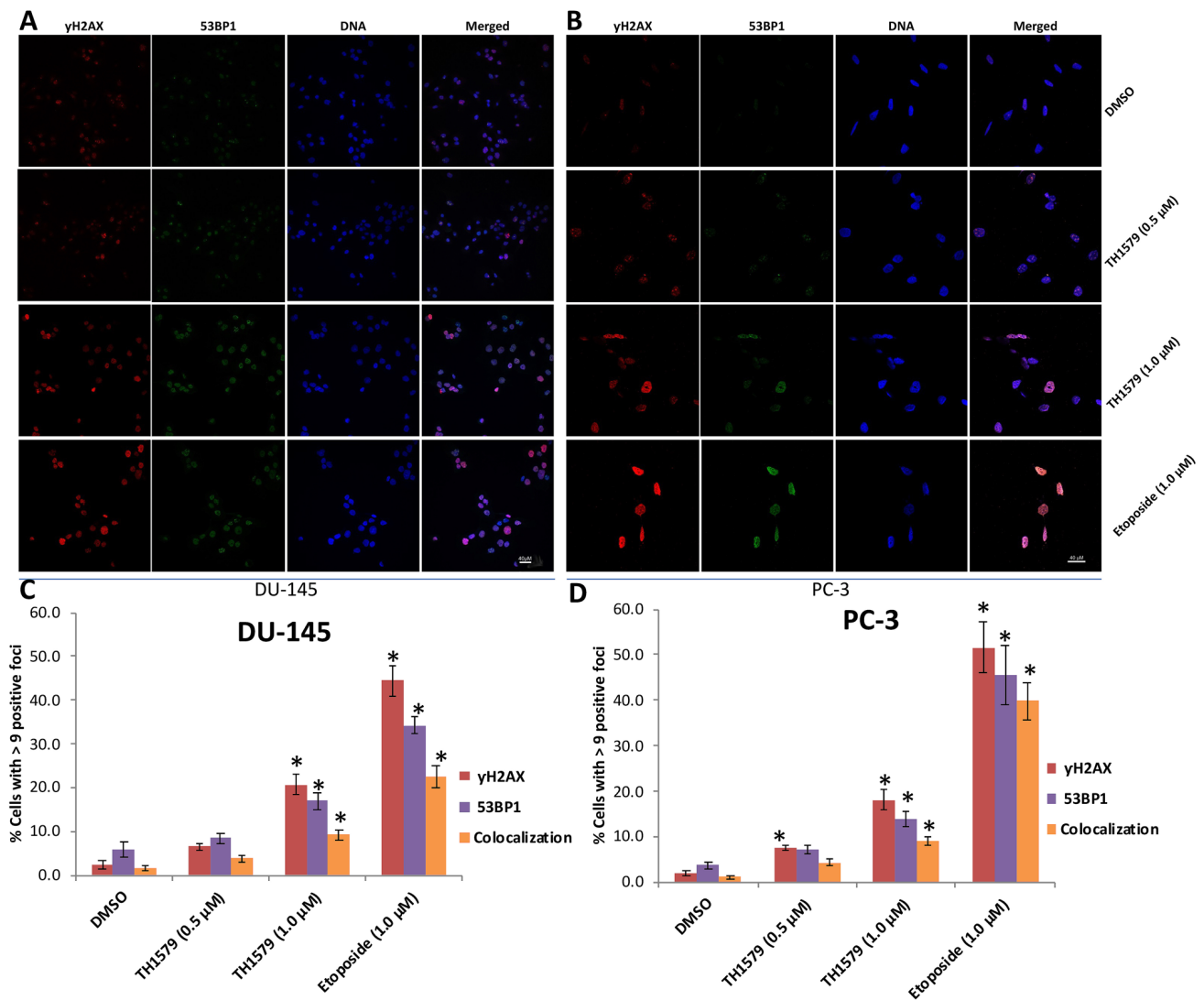


Figure 4. TH1579 promotes DNA double-strand breakage and DNA damage in castration-resistant prostate cancer cells, indicated by 53BP1 and γ H2AX foci. Representative immunofluorescence staining images of γ H2AX foci (red) and 53BP1 foci (green) accumulation in DNA and colocalisation in (A) DU-145 and (B) PC-3 cells 3 days after treatment with TH1579. DNA was counterstained with DAPI. Colocalisation of the red γ H2AX and green 53BP1 foci is indicated by yellow foci in the merged fields. Quantification of (C) DU-145 and (D) PC-3 cells with γ H2AX and/or 53BP1 positive foci after 72 h treatment with TH1579 or etoposide. Data are shown as Mean \pm SE from three independent experiments; ≥ 200 cells/sample. * $P < 0.01$, each experiment group including TH1579 (1.0 μ M), TH1579 (0.5 μ M) or Etoposide group vs. DMSO group; Tukey's test. 53BP1, p53-binding protein 1.

regulation of DNA repair. Moreover, the present study indicated that DU-145 cells are more sensitive to TH1579 treatment than PC-3 cells. This result suggested that the antitumour activity of TH1579 is associated with p53 status, as PC-3 cells, but not DU-145 cells, carry a p53 deletion mutation. Although this result is in agreement with that of a previous study (8), it may require further investigation.

Although MTH1 is required for the survival of cancer cells, the downregulation of MTH1 mRNA expression does not inhibit the proliferation of all cell lines (8). While certain studies have suggested genetic or phenotypic resistance mechanisms for this phenomenon, others have hypothesized that MTH1 is not required for the proliferation of all cancer cell types (8,18). Moreover, chemical inhibition of MTH1 with inhibitors such as TH1579 or TH588 is more efficient at suppressing tumour cell proliferation than siRNA-mediated silencing of MTH1 (18). A compensatory mechanism through the gradual exhaustion of MTH1 has been suggested to be

responsible for this phenomenon (18). Therefore, it can be inferred that chemical inhibition or gene silencing may not always be therapeutically effective for tumour treatment.

Another drawback of using TH1579 is that the inhibition of MTH1 function may increase spontaneous mutagenesis and carcinogenesis (35). However, these data were obtained using a mouse model; the time required to cause spontaneous mutagenesis and carcinogenesis in humans may be far longer. Given that most patients with advanced prostate cancer are over 70 years of age, this should not be a primary concern for their treatment compared with attempting to prolong their lifespan.

In conclusion, the results of the present study suggested that TH1579 may be a potential potent chemotherapeutic agent for treating patients with hormone-naïve prostate cancer or CRPC. Further studies are required to validate the antitumour activity and underlying molecular mechanisms of MTH1 inhibitors in human CRPC cells.

Acknowledgements

Not applicable.

Funding

The present study was funded by the Key Projects of Provincial Educational Department, Anhui Province, China Mainland (grant no. KJ2019A0373), and Bengbu Medical College, Anhui Province, China mainland (grant no. BYKC201912).

Availability of data and materials

The datasets used and/or analyzed during the current study are available from the corresponding author on reasonable request.

Authors' contributions

MH analyzed and interpreted the experiment data. JN, LM, YY and YW performed the western blotting, cellular viability, immunofluorescence and flow cytometry assay experiments. MH wrote the manuscript. All authors read and approved the final manuscript.

Ethics approval and consent to participate

Not applicable.

Patient consent for publication

Not applicable.

Competing interests

The authors declare that they have no competing interests.

References

- Wong MC, Goggins WB, Wang HH, Fung FD, Leung C, Wong SY, Ng CF and Sung JJ: Global incidence and mortality for prostate cancer: Analysis of temporal patterns and trends in 36 countries. *Eur Urol* 7: 862-874, 2016.
- Crawford ED, Higano CS, Shore ND, Hussain M and Petrylak DP: Treating patients with metastatic castration resistant prostate cancer: A comprehensive review of available therapies. *J Urol* 194: 1537-1547, 2015.
- van Dodewaard-de Jong JM, Verheul HMW, Bloemendaal HJ, de Klerk JMH, Carducci MA and van den Eertwegh AJM: New Treatment options for patients with metastatic prostate cancer: What is the optimal sequence? *Clin Genitourin Cancer* 13: 271-279, 2015.
- Jackson SP and Bartek J: The DNA-damage response in human biology and disease. *Nature* 461: 1071-1078, 2009.
- Hah SS, Mundt JM, Kim HM, Sumbad RA, Turteltaub KW and Henderson PT: Measurement of 7,8-dihydro-8-oxo-2'-deoxyguanosine metabolism in MCF-7 cells at low concentrations using accelerator mass spectrometry. *Proc Natl Acad Sci USA* 104: 11203-11208, 2007.
- Zhang Y, Du Y, Le W, Wang K, Kieffer N and Zhang J: Redox control of the survival of healthy and diseased cells. *Antioxid Redox Signal* 15: 2867-2908, 2011.
- Nakabeppu Y: Cellular levels of 8-oxoguanine in either DNA or the nucleotide pool play pivotal roles in carcinogenesis and survival of cancer cells. *Int J Mol Sci* 15: 12543-12557, 2014.
- Gad H, Koolmeister T, Jemth AS, Eshtad S, Jacques SA, Ström CE, Svensson LM, Schultz N, Lundback T, Einarsdottir BO, *et al*: MTH1 inhibition eradicates cancer by preventing sanitation of the dNTP pool. *Nature* 508: 215-221, 2014.
- Kennedy CH, Pass HI and Mitchell JB: Overexpression of human mutT homologue (hMTH1) protein as a marker of persistent oxidative stress in primary non-small cell lung tumors. *Free Radic Biol Med* 34: 1447-1457, 2003.
- Iida T, Furuta A, Kawashima M, Nishida J, Nakabeppu Y and Iwaki T: Accumulation of 8-oxo-2'-deoxyguanosine and increased expression of hMTH1 protein in brain tumors. *Neuro Oncol* 3: 73-81, 2001.
- Tu Y, Wang Z, Wang X, Yang H, Zhang P, Johnson M, Liu N, Liu H, Jin W, Zhang Y, *et al*: Birth of MTH1 as a therapeutic target for glioblastoma: MTH1 is indispensable for glioma tumorigenesis. *Am J Transl Res* 8: 2803-2811, 2016.
- Okamoto K, Toyokuni S, Kim WJ, Ogawa O, Kakehi Y, Arai S, Hiai H and Yoshida O: Overexpression of human mutT homologue gene messenger RNA in renal-cell carcinoma: Evidence of persistent oxidative stress in cancer. *Int J Cancer* 65: 437-441, 1996.
- Zhang X, Song W, Zhou Y, Mao F, Lin Y, Guan J and Sun Q: Expression and function of MutT homolog 1 in distinct sub-types of breast cancer. *Oncol Lett* 13: 2161-2168, 2017.
- Koketsu S, Watanabe T and Nagawa H: Expression of DNA repair protein: MYH, NTH1, and MTH1 in colorectal cancer. *HepatoGastroenterology* 51: 638-642, 2004.
- Akiyama S, Saeki H, Nakashima Y, Iimori M, Kitao H, Oki E, Oda Y, Nakabeppu Y, Kakeji Y and Maehara Y: Prognostic impact of MutT homolog-1 expression on esophageal squamous cell carcinoma. *Cancer Med* 6: 258-266, 2017.
- Rai P, Young JJ, Burton DG, Giribaldi MG, Onder TT and Weinberg RA: Enhanced elimination of oxidized guanine nucleotides inhibits oncogenic RAS-induced DNA damage and premature senescence. *Oncogene* 30: 1489-1496, 2011.
- Huber KV, Salah E, Radic B, Gridling M, Elkins JM, Stukalov A, Jemth AS, Gokturk C, Sanjiv K, Strömberg K, *et al*: Stereospecific targeting of MTH1 by (S)-crizotinib as an anticancer strategy. *Nature* 508: 222-227, 2014.
- Warpmann Berglund U, Sanjiv K, Gad H, Kalderén C, Koolmeister T, Pham T, Gokturk C, Jafari R, Maddalo G, Seashore-Ludlow B, *et al*: Validation and development of MTH1 inhibitors for treatment of cancer. *Ann Oncol* 27: 2275-2283, 2016.
- Kettle JG, Alwan H, Bista M, Breed J, Davies NL, Eckersley K, Fillery S, Foote KM, Goodwin L, Jones DR, *et al*: Potent and selective inhibitors of MTH1 probe its role in cancer cell survival. *J Med Chem* 59: 2346-2361, 2016.
- Petrocchi A, Leo E, Reyna NJ, Hamilton MM, Shi X, Parker CA, Mseeh F, Bardenhagen JP, Leonard P, Cross JB, *et al*: Identification of potent and selective MTH1 inhibitors. *Bioorg Med Chem Lett* 26: 1503-1507, 2016.
- Kawamura T, Kawatani M, Muroi M, Kondoh Y, Futamura Y, Aono H, Tanaka M, Honda K and Osada H: Proteomic profiling of small-molecule inhibitors reveals dispensability of MTH1 for cancer cell survival. *Sci Rep* 6: 26521, 2016.
- Scobie M, Helleday T, Koolmeister T, Jacques S, Desroses M and Jacques-cordonnier M: Pyrimidine-2,4-diamine derivatives for treatment of cancer. *WO2014084778*.
- Pudelko L, Rouhi P, Sanjiv K, Gad H, Kalderén C, Höglund A, Squatrito M, Schuhmacher AJ, Edwards S, Hägerstrand D, *et al*: Glioblastoma and glioblastoma stem cells are dependent on functional MTH1. *Oncotarget* 8: 84671-84684, 2017.
- Hua X, Sanjiv K, Gad H, Pham T, Gokturk C, Rasti A, Zhao Z, He K, Feng M, Zang Y, *et al*: Karonudib is a promising anticancer therapy in hepatocellular carcinoma. *Ther Adv Med Oncol* 11: 1758835919866960, 2019.
- Das I, Gad H, Brautigam L, Pudelko L, Tuminen R, Helleday T, Hansson J, Brage S and Berglund U: 1180 Effects of MTH1 inhibitor TH1579 on cutaneous melanoma. *J Invest Dermatol* 138: S200, 2018.
- Einarsdottir BO, Karlsson J, Söderberg EMV, Lindberg MF, Funck-Brentano E, Jespersen H, Brynjolfsson SF, Olofsson Bagge R, Carstam L, Carstam L, *et al*: A patient-derived xenograft pre-clinical trial reveals treatment responses and a resistance mechanism to karonudib in metastatic melanoma. *Cell Death Dis* 9: 810, 2018.
- Zhou W, Ma L, Yang J, Qiao H, Li L, Guo Q, Ma J, Zhao L, Wang J, Jiang G, *et al*: Potent and specific MTH1 inhibitors targeting gastric cancer. *Cell Death Dis* 10: 434, 2019.
- Lee JW, Lee S, Ho JN, Youn JI, Byun SS and Lee E: Antitumor effects of MutT homolog 1 inhibitors in human bladder cancer cells. *Biosci Biotechnol Biochem* 83: 2265-2271, 2019.

29. Carroll AG, Voeller HJ, Sugars L and Gelmann EP: p53 oncogene mutations in three human prostate cancer cell lines. *Prostate* 23: 123-134, 1993.
30. Mamidi TKK, Wu J and Hicks C: Integrating germline and somatic variation information using genomic data for the discovery of biomarkers in prostate cancer. *BMC Cancer* 19: 229, 2019.
31. Asim M, Tarish F, Zecchini HI, Sanjiv K, Gelali E, Massie CE, Baridi A, Warren AY, Zhao W, Ogris C, *et al*: Synthetic lethality between androgen receptor signalling and the PARP pathway in prostate cancer. *Nat Commun* 8: 374, 2017.
32. Popovics P, Schally AV, Szalontay L, Block NL and Rick FG: Targeted cytotoxic analog of luteinizing hormone-releasing hormone (LHRH), AEZS-108 (AN-152), inhibits the growth of DU-145 human castration-resistant prostate cancer in vivo and in vitro through elevating p21 and ROS levels. *Oncotarget* 5: 4567-4578, 2014.
33. Lorente D, Mateo J, Perez-Lopez R, de Bono JS and Attard G: Sequencing of agents in castration-resistant prostate cancer. *Lancet Oncol* 16: e279-292, 2015.
34. Knudsen KE: The AR-DNA repair axis: Insights into prostate cancer aggressiveness. *Can J Urol* 26 (5 Suppl 2): S22-S23, 2019.
35. Nakabeppu Y, Ohta E and Abolhassani N: MTH1 as a nucleotide pool sanitizing enzyme: Friend or foe? *Free Radic Biol Med* 107: 151-158, 2017.



This work is licensed under a Creative Commons Attribution-NonCommercial-NoDerivatives 4.0 International (CC BY-NC-ND 4.0) License.